On the changes in surface ozone over the twenty-first century: sensitivity to changes in surface temperature and chemical mechanisms

Alex T. Archibald[1,2], Steven T. Turnock[3],
Paul T. Griffiths[1,2], Tony Cox[1], Richard G. Derwent[4],
Christoph Knote[5] and Matthew Shin[1]

[1]Department of Chemistry, and [2]NCAS-Climate, University of Cambridge, Cambridge CB1 2EW, UK
[3]Met Office Hadley Centre, FitzRoy Road, Exeter EX1 3PB, UK
[4]rdscientific, Newbury, Berkshire RG14 6LH, UK
[5]Fakultät für Physik, Ludwig-Maximilians-Universität München, Theresienstr. 37, 80333 München, Deutschland

ATA, 0000-0001-9302-4180; STT, 0000-0002-0036-4627;
PTG, 0000-0002-1089-340X; CK, 0000-0001-9105-9179;
MS, 0000-0001-7235-6127

Author for correspondence:
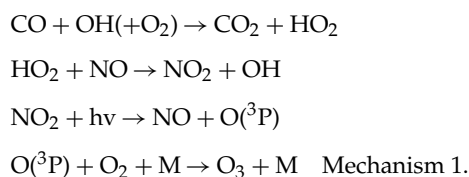Alex T. Archibald
e-mail: ata27@cam.ac.uk

In this study, we show using a state-of-the-art Earth system model, UKESM1, that emissions and climate scenario depending, there could be large changes in surface ozone by the end of the twenty-first century, with unprecedentedly large increases over South and East Asia. We also show that statistical modelling of the trends in future ozone works well in reproducing the model output between 1900 and 2050. However, beyond 2050, and especially under large climate change scenarios, the statistical model results are in poorer agreement with the fully interactive Earth system model output. This suggests that additional processes occurring in the Earth system model such as changes in the production of ozone at higher temperatures or changes in the influx of ozone from the stratosphere, which are not captured by the statistical model, have a first order impact on the evolution of surface ozone over the twenty-first century. We show in a series of idealized box model simulations, with two different chemical schemes, that changes in temperature lead to diverging responses between the schemes. This points at the chemical

mechanisms as being a source of uncertainty in the response of ozone to changes in temperature, and so climate, in the future. This underscores the need for more work to be performed to better understand the response of ozone to changes in temperature and constrain how well this relationship is simulated in models.

This article is part of a discussion meeting issue 'Air quality, past present and future'.

1. Introduction

Tropospheric ozone is a key component of air pollution (e.g. [1]). It is formed through a complex series of photochemical reactions that involve cycles which couple the nitrogen oxides ($NOx = NO + NO_2$) and hydrogen oxides ($HOx = OH + HO_2$) and is mediated by volatile organic compounds (VOCs). The most basic mechanism, where carbon monoxide (CO) represents a VOC, is outlined below

$$CO + OH(+O_2) \rightarrow CO_2 + HO_2$$

$$HO_2 + NO \rightarrow NO_2 + OH$$

$$NO_2 + hv \rightarrow NO + O(^3P)$$

$$O(^3P) + O_2 + M \rightarrow O_3 + M \quad \text{Mechanism 1.}$$

This mechanism (Mechanism 1) is a simplification of the complex chemistry that occurs in the troposphere. It fails to account for some of the important features recorded by observations made in the field, which include (1) titration of ozone, and a reduction in the rate of ozone production, at high levels of NOx; and (2) an increase in ozone with increasing temperature. The increase in levels of surface ozone with increasing temperature has been known for several decades with early studies focused on analysing ozone pollution events during summer heat waves [2]. As an example, figure 1 shows data for the ozone-temperature relationship during three summer heat wave events in the southeast of the UK.

These data (figure 1) show the typical trends of increases in ozone levels with increasing temperature, seen in many places around the world (e.g. the northeast USA [3]). As temperature increases above 290 K there are large increases in surface ozone. Figure 1 also illustrates that there is a decrease in the maximum levels of ozone and a decrease in the gradient of the ozone-temperature relationship over time; the ozone values recorded during the 1976 heat wave were substantially higher than those recorded in 2003 and the 2003 values [4] were higher than those observed in 2018. This decrease in the maximum ozone values over time is also well observed across western Europe ([5] and references therein) and the USA ([6] and references therein) and is related to the general decreasing trends in emissions of ozone precursors over time [7]. What is less clear is the cause of the trend in the ozone-temperature gradient, but there are likely to be several factors.

The increase in ozone with increasing temperature (shown in figure 1) has been ascribed to several causes in the literature. These were recently comprehensively reviewed by Fu & Tian [8] and Porter & Heald [9]. By decomposing the rate of change of the ozone mixing ratio ($[O_3]$) with temperature (T) using the chain-rule, an analytical expression can be generated which encompasses the drivers for the change in ozone with temperature [3]:

$$\frac{d[O_3]}{dT} = \frac{\delta[O_3]}{\delta[\text{stagnation}]} \times \frac{d[\text{stagnation}]}{dT} + \frac{\delta[O_3]}{\delta[\text{chemistry}]} \times \frac{d[\text{chemistry}]}{dT}$$
$$+ \frac{\delta[O_3]}{\delta[\text{emissions}]} \times \frac{d[\text{emissions}]}{dT}. \tag{1.1}$$

This expression (equation (1.1)) is similar in form to the continuity equation for ozone, which relates the temporal behaviour of ozone (($d[O_3])/dt$) to terms related to (1) transport (the first
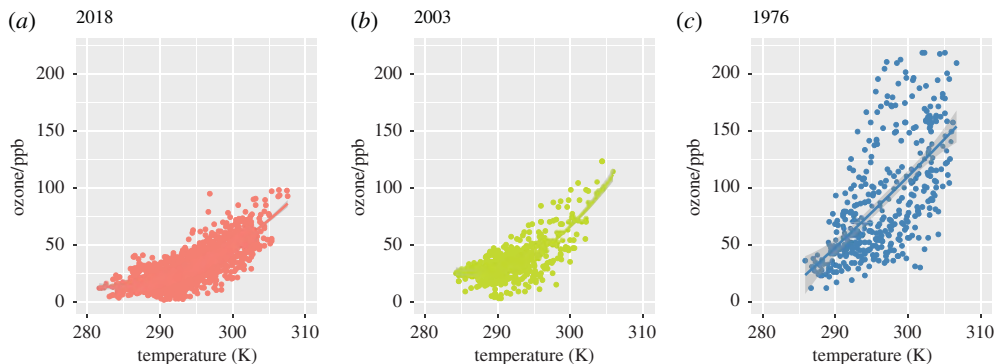
Figure 1. Comparison of hourly average surface ozone and temperature data obtained during heat wave periods in the southeast UK. (*a*) Data from 2018; (*b*) from 2003; (c) from 1976. The highest levels of ozone have decreased going forward in time in spite of increases in the maximum temperature with time. The ozone data for 1976 and 2003 are from the Harwell observatory and for 2018 from the Wicken Fen observatory (as Harwell was non-operational). Temperature data are from Heathrow for all years. The mismatch in location of ozone and temperature data is not ideal but unavoidable and during these conditions the heat wave was very extensive such that temperatures are expected to have been very similar at the ozone sites. Best fit lines using a LOESS function in ggplot are added to each panel as a guide only. (Online version in colour.)

term in equation (1.1)) (2) chemistry and (3) emissions [10]. The stagnation term reflects the slowing down of air, which is common under high pressure conditions which temperature extremes are associated with, changes in relative humidity and deposition of ozone.

Equation (1.1) incorporates the change in ozone precursor emissions with temperature and the change in chemistry with temperature as two important drivers for the effect of temperature on ozone. The change in chemistry with temperature is largely driven by an increase in the rate coefficients for chemical processes, which is driven by the presence of positive activation energy barriers for chemical reactions [11]; although it should be noted that several important processes in the atmosphere have rate coefficients that decrease with increasing temperature [12]. An increase in temperature can also enable different pathways to be accessed on the potential energy surface the reactant(s) occupies—pathways which may result in a greater propensity for producing ozone [13].

The effect of temperature on reactions in the atmosphere has been well studied (see [8]). For instance, a strong temperature dependence is observed for the rate constant for reaction between OH and methane (CH_4), which increases by a factor of 16 from 200 to 300 K [14]. This provides a globally important source of peroxy radicals (RO_2) which mediate the formation of ozone in the troposphere [1].

Another important reaction in mediating ozone at regional scales is the thermal decomposition of peroxyacetic nitric anhydride ($CH_3C(O)O_2NO_2$), commonly known by its misnomer peroxyacetyl nitrate (PAN) [15]. PAN is formed from more complex VOCs than methane, such as isoprene, and is a major reservoir for NOx [15,16]. Figure 2*a* shows that the lifetime for first order decomposition of PAN changes dramatically with increasing temperature. At higher temperatures, the PAN lifetime becomes shorter and decomposition of PAN into peroxy acetyl radicals ($CH_3C(O)O_2$) and NO_2 more rapid:

$$PAN \ CH_3C(O)O_2 + NO_2. \tag{1.2}$$

Thus, at high temperatures PAN goes from being a reservoir to a source of NOx, which can go on to increase the rate of ozone production as seen in Mechanism 1. As a result of the increase in reaction rates and decrease in the lifetime of NOx reservoirs, increases in temperature lead to increases in the rate of ozone production [8,9].
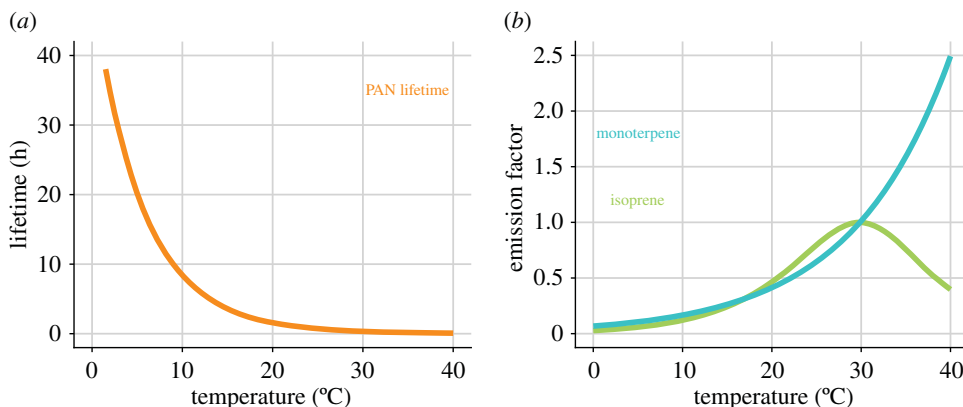
Figure 2. Comparison of the lifetime of PAN (*a*) and the emission factors of isoprene and monoterpenes (*b*) as a function of temperature. (Online version in colour.)

Probably more important for the ozone-temperature relationship, and especially in the case of the data in figure 1, are changes in VOC emissions with temperature. Figure 2*b* shows that at higher temperatures the rate of emissions of important ozone precursors produced from vegetation, like isoprene, increases significantly, doubling from 20°C to 30°C for isoprene [17]. Lee *et al.* [4] attributed a significant fraction of the increase in ozone in the southeast UK in 2003 (figure 1*b*) to an increase in VOC emissions during the heat wave. Importantly it is not only vegetation emissions that increase with temperature but there is strong evidence for increases of anthropogenic VOC emissions at higher temperatures too [18]. Combined, these temperature-driven increases in emissions of ozone precursors will lead to increases in ozone as temperatures increase [8].

Assessment of the risks associated with future climate change requires consideration not only of the mean climate state, but also less frequent but more impactful events [19]. Figure 1 shows data for recorded extreme ozone events—periods in which there was a prolonged increase in temperature accompanied by meteorological stagnation that lead to increased ozone production and suppressed removal. The complex nonlinear chemistry of ozone makes it very difficult to attribute the drivers of the severity and frequency of these events. To unpick which processes are most important for increasing surface ozone to dangerous levels requires the use of numerical models for impact assessment studies. A key question then is to use models to assess how the magnitude and frequency of these high impact events may change.

In this paper, we explore the effects of changes in emissions, climate and temperature on ozone through an analysis of two sets of model simulations. Firstly, with the new UK Earth system model (UKESM1) [20], which has been run as part of the Coupled Model Intercomparison Project phase 6 (CMIP6). CMIP6 [21] is an international effort to coordinate research into the Earth system. It provides the key underpinning information which will enable the next IPCC report to be compiled. We explore seven different estimates of the evolution of future climate and ozone precursor emission changes from 2015 to 2100 in simulations performed as part of CMIP6. We compare the results of these simulations with the fully interactive UKESM1 model to those from a statistical model trained on the output of simulations performed as part of the Hemispheric Transport of Air Pollution phase 2 (HTAP_Param) [22,23]. Comparing the results from UKESM1 and the HTAP_Param enables an assessment of the changes in ozone attributed to factors other than ozone precursor emissions changes, i.e. climate-driven changes. Secondly, we compare the results of idealized box model simulations run with different chemical mechanisms (used in chemistry-climate and Earth system models) to explore the sensitivity that these different mechanisms have to changes in temperature. This allows for an assessment of the sensitivity of the ozone-temperature relationship to the choice of chemical mechanisms used in state-of-the-art models.

This paper is organized as follows: In §2, we describe the UKESM1 model set-up and methods used in our box model simulations. In §3, we discuss the results of the UKESM1 future projections of surface ozone change while, in §4, we discuss the sensitivity studies with the simple box model. In §5, we summarize and conclude our study.

2. Methods

The UKESM1 is a state-of-the-art fully coupled Earth System model [20]. It includes interactive and dynamic modules to simulate the ocean and sea ice, including the ocean carbon cycle, the physical atmosphere, the land surface (and terrestrial vegetation and the carbon cycle) and, of most importance to the present study, atmospheric chemistry and aerosols (using the UKCA sub-model [24]). The model has been run as part of CMIP6 [21] and is discussed in detail by Sellar *et al.* [20] with the forcings used in the CMIP6 simulations discussed in Sellar *et al.* [25]. Here, we make use of simulations from the CMIP6 Historical simulation [21] and the ScenarioMIP simulations [26]. The Historical simulation provides boundary conditions, including greenhouse gas and ozone precursor emissions and their trends, for CMIP6 models to simulate the recent past change in ozone (*ca.* 1850–2014), while the ScenarioMIP simulations project future changes and supply boundary conditions, greenhouse gas trajectories and ozone precursor emission changes, which cover the period 2015–2100 using the shared socioeconomic pathways (SSP) scenarios. In this study we have made use of a number of different ensemble members of UKESM1. These ensemble members are produced by starting the model simulation with slightly different initial conditions, taken from the spun-up pre-industrial climate control run and spanning different climate states (El Nino Southern Oscillation, North Atlantic Oscillation, Quasi-Biennial Oscillation, etc.), to allow each ensemble member to evolve independently and so enable an estimate of the internal variability of the model system. Table 1 lists the experiments analysed here and gives an indication of the levels of climate change and air pollution trajectories simulated.

In addition to the UKESM1 model results, we also make use of a statistical model of ozone changes which relates the ozone mixing ratio at the surface to the underlying ozone precursor emissions. The change in ozone (ΔO_3) is calculated by:

$$\Delta O_3(k) = \sum_{i=1}^{3} \sum_{j=1}^{5} f_{i,j} \Delta O_{3e}(i,j,k) + f_m \Delta O_{3m}(k), \qquad (2.1)$$

where $\Delta O_3 =$ monthly mean ozone response (ΔO_{3e} - to emission precursors, $\Delta O_3 m$ - to global CH_4 concentrations); $k =$ receptor region; $i =$ individual precursor emission (NOx, CO and NMVOCs); $j =$ emission source region; $f =$ emission scaling factor (linear for changes in CO and NMVOCs but nonlinear for NO_x and CH_4)

This statistical model (HTAP_Param) was developed by Turnock *et al.* [22] based on emulating the response of modelled ozone to emission perturbations to determine the sensitivity of ozone to changes in global CH_4 abundance and emissions of CO, VOCs and NOx by fitting the output from simulations performed as part of the HTAP-2 multi model study [27]. As such the results from UKESM1 are independent from the HTAP_Param as UKESM1 was not used in the HTAP-2 multi model study [27]. The HTAP_Param uses the fractional change in global CH_4 abundance and precursors emissions (NOx, CO and VOCs) for a specific scenario to scale the simulated ozone response from each individual HTAP-2 model. For CO and VOCs the calculated fractional emission change is used directly as a linear scaling factor, whereas for CH_4 and NOx a nonlinear scaling factor is used. The total ozone response from the HTAP_Param is obtained by summing up the changes from individual input models to all the precursor emissions across source regions. The HTAP_Param provides a rapid way of assessing the global and regional mean changes in tropospheric ozone to different emission perturbation scenarios. Further details on the HTAP_Param are provided in Turnock *et al.* [22,23].

A feature of chemistry-climate modelling intercomparisons (like CMIP6) is that ozone at the surface is highly variable across models (e.g. [28,29]). However, attributing the cause of model

Table 1. Details of the UKESM1 simulations analysed.

scenario	number of ensemble members	climate change scenario	air pollution trajectory	start-end year
historical	9	historical changes	historical changes	1850–2014
SSP1–19	5	low	low	2015–2100
SSP1–26	5	low	low	2015–2100
SSP2–45	5	medium	medium	2015–2100
SSP3–70	5	high	high	2015–2100
SSP4–34	5	medium	high	2015–2100
SSP5–34	5	medium	low	2015–2100
SSP5–85	5	high	low	2015–2100

variability is challenging and not a major focus of these studies. Wild *et al.* [30] highlight the importance of a range of different physical and emissions parameters, including deposition, in contributing to uncertainty in tropospheric ozone from an ensemble of three models. They highlight that these models have different sensitivities to the ozone precursor emissions and deposition rates but did not probe the sensitivity and variability that is attributed to mechanistic uncertainty. As such it remains one hypothesis that a large source of model variability in surface ozone comes from the use of different chemical mechanisms which may have different sensitivities to climate. In particular, several studies have highlighted that uncertainty in the oxidation of isoprene is important (e.g. [31,32]). We show results of temperature sensitivity experiments performed using representative chemistry schemes from typical chemistry-climate models. By their nature chemistry-climate models (and therefore Earth system models) use mechanisms which have reduced complexity (numbers of species and reactions) compared with reference schemes. Some chemical data are missing: competing requirements necessitate a reduced mechanism of low computational cost, while the nonlinear and strongly coupled chemistry make it necessary to adopt as few approximations as is reasonable to capture the role of key intermediates and reservoir species, such as aldehydes and nitrates, which are important at regional scales. Zero-dimensional or 'box' model experiments were performed using the BOXMOX modelling framework [33,34], using the MOZART-4 (Model for OZone and related chemical tracers) chemical mechanism [35] and UKCA StratTrop chemical mechanism (the chemistry scheme used in UKESM1 [24]). We isolated the uncertainty arising from the choice of mechanism by focusing on a globally important but short-lived VOC, isoprene, and its ozone production in the presence of NOx.

The box model simulations used conditions appropriate to the dry planetary boundary layer: a pressure of 1000 hPa, with background mixing ratios of 1% H_2O, 1750 ppb CH_4, 500 ppb H_2, 120 ppb CO, 30 ppb O_3. Temperature, and the initial amounts of NOx and isoprene, were varied systematically resulting in a total of 100 simulations run. The photolysis rate constants were kept constant between experiments and varied diurnally, with noontime values for $J(O(^1D))$ of $3.6 \times 10^{-5} \, s^{-1}$ and $J(NO_2)$ of $1.1 \times 10^{-2} \, s^{-1}$. Deposition of reservoir species was incorporated to represent conditions typical of the boundary layer. The simulations were run for 4 days, with the output analysed at noon on the fourth day. Simulations were performed across a range of temperatures (273, 293, 313 K) with temperature held constant throughout the simulations.

3. The effect of future changes in climate and emissions on surface ozone

Figure 3 shows the results from UKESM1 for the Historical and ScenarioMIP simulations and shows 200 years of the evolution of surface ozone at global and regional scales. UKESM1 has
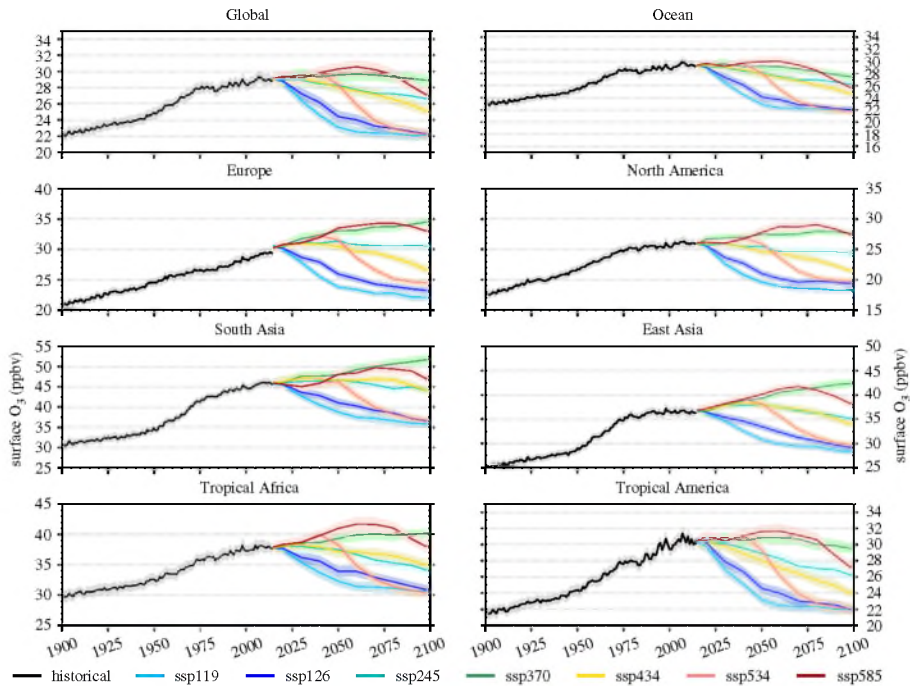
Figure 3. The evolution of surface ozone at different locations across the globe as modelled by the UKESM1 model from 1900 to 2100. The black line refers to the results from the mean of the CMIP6 Historical simulations, while the coloured lines represent the various ScenarioMIP scenarios for future climate and ozone evolution (see legend for the details of each scenario). Note that different *y*-axis scales are used in each sub-plot. Solid lines are used to indicate the ensemble mean and shading ±1 s.d. (Online version in colour.)

undergone rigorous evaluation against surface observations [20,24,36]. Figure 3 splits the analysis of annual average ozone into a number of regions. These include North America, Europe, South and East Asia, defined by the HTAP2 protocol (e.g. [23]), as well as the tropics in Africa (30° S to 30° N, 0° to 45° E) and the Americas (30° S to 30° N, 75° W to 30° W), over the oceans and the global surface.

In general, surface ozone in the UKESM1 model is underpredicted in the winter and overpredicted in the summer, which leads to very low annual mean biases when compared with observations from the TOAR database [37] of global surface ozone [24]. The TOAR database allows for comprehensive evaluation of surface ozone over the European, North American and East Asian regions shown in figure 3 but a lack of observational data prohibits rigorous evaluation in the other locations. Consistent with other CMIP6 modelling studies (e.g. [36,38]), UKESM1 shows that global mean surface ozone increased steadily throughout the twentieth century (approx. 28% increase over the period 1900–2000), driven by increases in the underlying emissions of ozone precursors in the troposphere, reaching a peak value around the year 2000 and showing some sign of decline between 2000 and 2014. Ozone levels in the model are controlled by a balance between *in situ* photochemical production and loss, as well as physical deposition at the surface and transport from the stratosphere. The chemistry involved is a complex series of coupled chemical processes, much more complex then outlined in Mechanism 1 and the representation of this chemistry is far from simple.

Our model simulations are averaged over broad geographical areas so are representative of large-scale changes. Schnell *et al*. [39] highlight that while models with the spatial resolution of UKESM1 may not be appropriate for simulating ozone events at very fine scales they are good at capturing regional-scale events (such as those associated with regional-scale heat waves). Our

analysis focuses on annual average surface level ozone. Annual averages (or monthly averages) are commonly used in the chemistry-climate modelling community (e.g. [28,36]) but are less widely used in the impacts community, where metrics like accumulated ozone over a threshold of 40 ppb during daylight hours (AOT40) and the maximum daily average 8-h running mean (MDA8) are preferred. Due to the non-Gaussian nature of pollution events the annual mean ozone will tend to under-represent the effects of extreme events but given its wide use in the chemistry-climate modelling community we adopt its use here.

Figure 3 shows an envelope for the spread (±1 s.d.) of the ensemble members and highlights that there is very little spread from ensemble members compared with the spread that results from different emissions and climate scenarios. From 2015 onwards the evolution of surface ozone is very dependent on the SSP scenario simulated. The SSP scenarios cover a wide range of metrics including global energy demand, population and GDP change as well as the corresponding changes in emissions of climate and air pollution gases and aerosols [26]. Table 1 summarizes the air pollution and climate emissions in these SSPs but briefly each SSP is identified by a socioeconomic trajectory (X) and a climate forcing (YY). The socioeconomic trajectories are: (1) sustainability, (2) middle of the road, (3) regional rivalry, (4) inequality and (5) fossil-fuel development. These scenarios can be qualitatively translated into the levels of emissions in table 1 and highlight, for example, that SSP1–19 indicates the socioeconomic trajectory 1 (sustainability with low emissions of air pollutants and climate forcing agents) and a climate forcing at 2100 with 1.9 W m^{-2} imbalance relative to the pre-industrial—e.g. a very modest change in climate forcing and strong control on ozone precursor emissions.

SSP1–19, which simulates wide adoption of climate mitigation measures and air quality controls, results in surface ozone levels at 2100 which are lower than those simulated during the 1900–1930s period in the historical run. However, SSP3–70 and SSP5–85 (high climate forcing scenarios) both end up with high levels of surface ozone globally (greater than 2 ppb above present day (2014) values (approx. 8% increase)). The evolution of surface ozone is not the same as surface temperature (not shown). As with other CMIP6 models, UKESM1 simulates that SSP5–85 results in a greater increase in surface temperature than SSP3–70 [40]. However, SSP3–70 results in approximately 2 ppb higher levels of ozone by the end of the twenty-first century than SSP5–85. This difference between these two high-risk scenarios is exacerbated regionally, especially in East and South Asia where the difference in ozone is as high as approximately 5 ppb by 2100. The cause of the differences in ozone between these different SSP simulations is partly linked to the very large difference in methane in these SSPs (SSP3–70 has the highest methane trajectory of all SSP scenarios), which is associated with the underlying assumptions of air quality/climate control which go into the SSP scenarios (table 1).

The mean surface ozone mixing ratio in figure 3 also shows significant variability geographically. Surface ozone is consistently highest in South and East Asia, and South Asia ends up being the worst place in the world for surface ozone by 2100 in SSP3–70. Unfortunately, few historic observations of surface ozone exist in South Asia, limiting our understanding of the fidelity of the model simulations in this important region [41].

Generally speaking, the UKESM1 results suggest that levels of surface ozone over the ocean are lower than those averaged globally and are lower than any of the land-based regions focused on in figure 3. Over the ocean there are few direct sources of ozone precursors and typically the oceans are major sinks of tropospheric ozone at the surface, owing to high levels of HOx [42]. Ozone increases over the ocean will be largely driven by emission-driven production over the land and advection of this ozone to the ocean or an increase of ozone transport from the stratosphere. As an example, Abalos *et al.* [43] (and references therein) have shown that the transport of ozone from the stratosphere (stratosphere troposphere transport (STT)) is enhanced in the future due to changes in atmospheric circulation—particularly changes in the Brewer–Dobson circulation in the lower stratosphere and the Hadley cell in the upper troposphere. In their study focusing on multi model simulations, Albalos *et al.* [43] attributed these changes to increases in greenhouse gases in the future scenarios they investigated and noted that at higher levels of greenhouse gas forcing (warming) the trend for increased STT was increased.
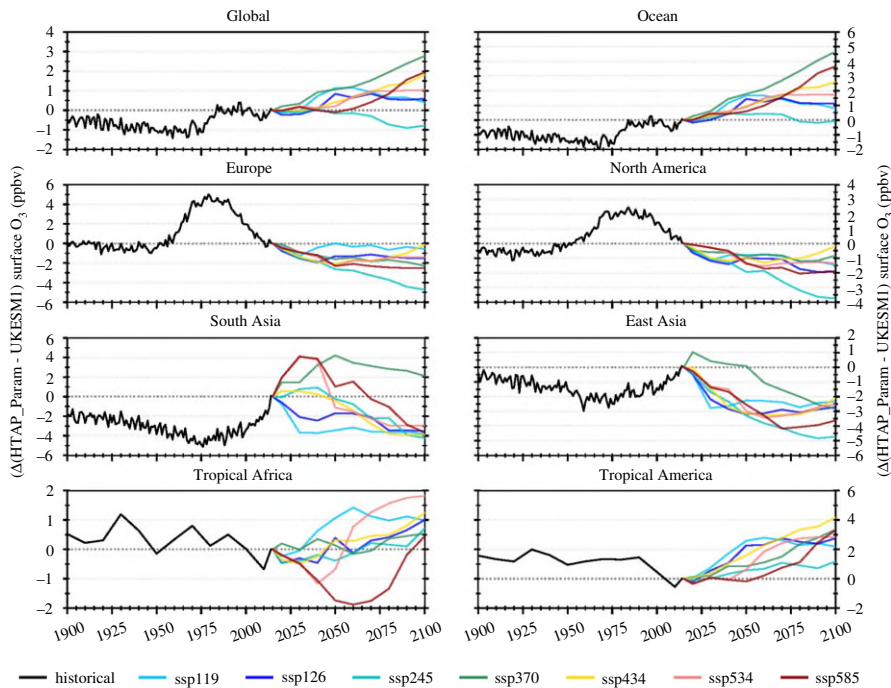
Figure 4. The difference in the evolution of surface ozone at different locations across the globe from 1900 to 2100 between the HTAP_Param statistical model and the UKESM1 simulations (positive values indicate an overestimate by the statistical model). The same colours are used as in figure 3 for consistency and the differences are calculated relative to the ensemble mean values in figure 3. (Online version in colour.)

The HTAP_Param enables a complementary prediction of surface ozone based on the same underlying emissions of ozone precursors as used in the UKESM1 simulations (figure 3). As the HTAP_Param is derived from emulation of global model results it is possible to quantify the uncertainty in the predictions it produces and Turnock *et al*. [23] calculate this to be 0.9 ppb. This uncertainty is similar in size to the uncertainty from the ensembles of the UKESM1 simulations (figure 3 envelopes), which is derived from the natural variability in the climate system.

Turnock *et al*. [23] show that the HTAP_Param performs well against the UKESM1 model simulations between 1750 and 2050. Here, we extend their analysis and evaluate the performance of the HTAP_Param against the UKESM1 simulations out to 2100. Figure 4 shows that while the performance of the HTAP_Param at the global average scale is very good in the historical period (within the 0.9 ppb uncertainty of HTAP_Param), there are points in time where the HTAP_Param over- and underestimates the levels of ozone simulated by UKESM1. Most notably during the period 1975–2000 where HTAP_Param predicts ozone levels 2 and 4 ppb higher than UKESM1 across North America and Europe, respectively. However, in many of the future SSP scenarios and in many more regions, in particular over South and East Asia, there are large differences between the HTAP_Param and UKESM1 simulations, especially from 2050 to 2100. This suggests that factors other than emissions, such as climate change and the associated changes in transport and temperature, have a significant impact on tropospheric ozone in the future.

As there have only been modest changes in climate over the historic time period, the difference between HTAP_Param and UKESM1 suggests that there are some biases between the HTAP_Param and UKESM1 which are independent of any climate change-related factors (i.e. related to structural biases in the model such as difference in VOC-NOx-O_3 sensitivity in the UKESM1 chemical mechanism). Turnock *et al*. [38] compare simulations from UKESM1 and other CMIP6 models and highlight that UKESM1 tends to be the least sensitive model of those analysed

in terms of the response of surface ozone to changes in VOC and NOx emissions over the historic period.

More striking, however, is the disagreement between HTAP_Param and UKESM1 at 2100. At the global scale, there is a clear pattern that the higher climate-forcing SSP scenarios (SSP4–34, SSP5–34, SSP3–70 and SSP5–85) result in the largest disagreement between UKESM1 and HTAP_Param, with HTAP_Param simulating ozone that is 1–3 ppb higher than the UKESM1 simulations at the global mean level. This pattern is also mirrored but exacerbated when the results are compared over the ocean, with biases increasing to approximately 5 ppb—biases which are greater than the projected changes in ozone averaged over the oceans in UKESM1 throughout the period 1900–2100 (figure 3).

The HTAP_Param is designed as a simple model to help in assessing future emission pathways. While Turnock *et al*. [23] have shown it has great utility, we show here that there are limitations. The overestimation of ozone in HTAP_Param relative to UKESM1 seen over the oceans and at the global scale is not seen over land in all regions analysed. Over many land areas HTAP_Param underestimates the surface ozone simulated by UKESM1—in East Asia this underestimation is approximately 5 ppb by 2100 (approx. 50% of the change between 1850 and 2000; figure 3). There are several likely causes of the underestimation of ozone by HTAP_Param with the most likely ones being changes in STT and the ozone-temperature effect, including the effects on ozone dry-deposition. Further work is required to identify the exact causes, but we suggest that additional terms to deal with the effect of climate change on surface ozone be added to models like HTAP_Param to increase their utility for simulating ozone under scenarios of strong climate change.

4. Uncertainty in the effects of temperature on ozone photochemistry

The comparison between the UKESM1 results and HTAP_Param highlight the importance of non-emission terms on the evolution of ozone over the twenty-first century. One cause of the disagreement could be the lack of temperature and related effects in the HTAP_Param. Here, we explore an aspect of this hypothesis by simulating the impacts of temperature changes on ozone using a simple box model run with two different chemical mechanisms [33]. The aim of the simulations are to determine if the ozone levels simulated by the different chemical mechanisms have different sensitivities to changes in temperature. We will use the simulations to quantify if the chemical mechanisms themselves are a source of uncertainty in the future evolution of ozone under changing temperature.

Figure 5 shows the results from box model simulations using two different chemical mechanisms run at two different temperatures (see §2 for details of the mechanisms and model set-up). Panels (a) and (c) display the results from the UKCA mechanism (used in UKESM1) and (b) and (d) display results from the MOZART-4 mechanism. Broadly speaking, both mechanisms display the same behaviour; as the concentration of VOC (isoprene) and NOx increase in the simulation the ozone-mixing ratio increases (e.g. [1]). However, there are differences between the mechanisms, which are evident when comparing panels (a) and (b) and (c) and (d). The gradient of the ozone increase is much less pronounced in UKCA (panel (a or c)) than in MOZART-4 (panel (b or d)). As temperature is increased, both mechanisms simulate higher levels of ozone—in broad agreement with the ozone-temperature relationship seen in observations (figure 1; [8]).

Figure 6 shows the difference in ozone with temperature ($\Delta O_3 / \Delta T$) in the box model runs. Panels (a) and (b) show the differences in ozone for the UKCA and MOZART-4 mechanisms between 293 and 273 K. In both cases the simulations run at the higher temperature result in more ozone. Comparing panels (a) and (b) highlights that the MOZART-4 mechanism simulates greater ozone production for this change in temperature (293–273 K) than the UKCA mechanism, which is shown to be very insensitive to these changes in temperature. Panels (c) and (d) (313 K versus 293 K) show that the increase in ozone is much larger at higher temperatures, mirroring the steep gradients in the ozone-temperature response seen in figure 1. Additionally, figure 6 highlights that the response of ozone simulated with the different mechanisms to changes in temperature are
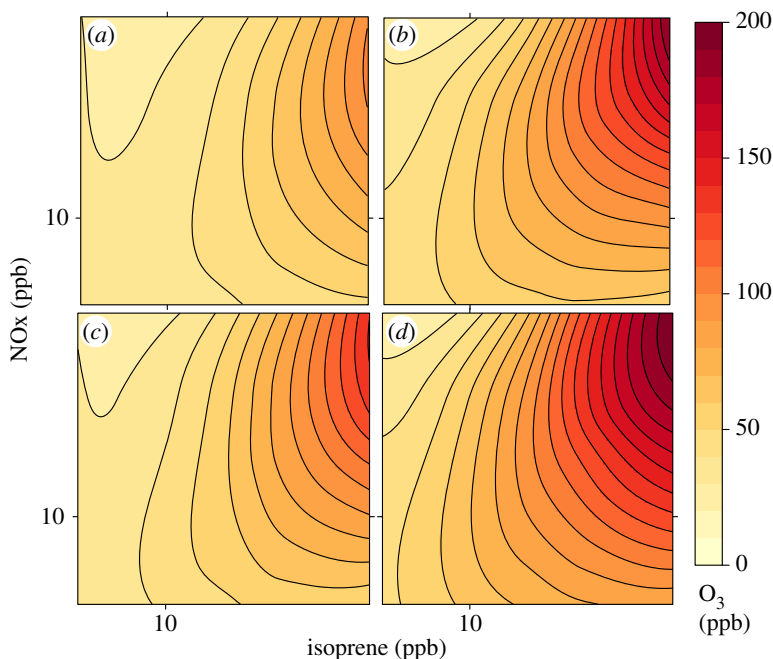
Figure 5. Box model simulations of the evolution of ozone as a function of isoprene and NOx using the UKCA mechanism (as used in UKESM1) (*a,c*) and the MOZART-4 mechanism (*b,d*). (*a,b*) Results for simulations run at 273 K. (*c,d*) Results for simulations run at 313 K. (Online version in colour.)

nonlinear in the range of [VOC] and [NOx] considered. The increases in ozone with temperature in UKCA tend to follow the same contours as the background ozone-mixing ratios (figure 5) across all temperatures investigated, whereas the MOZART-4 mechanism results in increases in ozone with temperature which do not map onto the underlying contours of the underlying ozone-mixing ratio (figure 5). Figure 6*d* shows that between 313 and 293 K the largest increases in ozone using the MOZART-4 mechanism are occurring independent of NOx (i.e. the ozone changes are appearing as an almost vertical line with no gradient along the y-axis). Analysis of changes in ΔPAN/ΔT (not shown) show broadly similar results between the mechanisms. There are large decreases in PAN at higher temperature while the PAN increases with increasing VOC and NOx. The similarity in ΔPAN/ΔT between the mechanisms but differences in $\Delta O_3/\Delta T$ suggest that PAN is not a controlling factor.

Rasmussen *et al*. [3] show in observations in the USA that $\Delta O_3/\Delta T$ reaches 6 ppb/K in parts of the USA in the summer—much higher than the levels we have simulated with the box model. Doherty *et al*. [44] show in global chemistry-climate model simulations that at regional scales $\Delta O_3/\Delta T$ is much smaller, suggesting that the large values for this relationship are dependent on a number of factors (some of which are likely to be very local/location-dependent) beyond the effect of temperature on chemistry. However, it is clear from figure 6 that there will be variability in model simulations of the ozone-temperature relationship that are driven by the underlying mechanisms themselves.

5. Discussion and conclusion

To understand what may happen to surface ozone in the future we require models capable of simulating the complex chemical and dynamical processes at play in the atmosphere. Figure 3 highlights that there is a large spread in projections of the evolution of ozone at the surface over the twenty-first century generated with the UKESM1 model. There are several scenarios
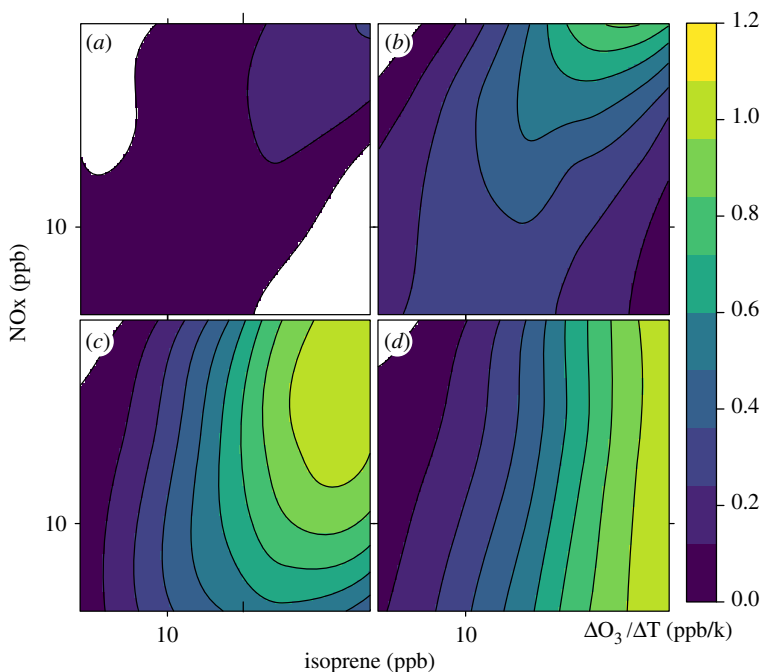
Figure 6. The effect of temperature on the box model simulations shown in figure 5 for the UKCA mechanism (as used in UKESM1) (*a,c*) and the MOZART-4 mechanism (*b,d*). (*a,b*) The change in ozone for simulations run at 293 and 273 K. (*c,d*) The change in ozone for simulations run at 313 and 293 K. All panels show the change in ozone divided by the change in temperature ($\Delta O_3/\Delta T$). (Online version in colour.)

in which levels of surface ozone may drop down to levels seen in the 1930s by 2100 but similarly there are scenarios in which ozone is projected to increase significantly by 2100. SSP3–70 is a plausible scenario for the future, but one which assumes very limited emissions mitigation in respects to both air quality and climate change, and so one we feel is a worst case scenario. We show here, in figure 3, that South and East Asia are regions which are particularly at threat of seeing unprecedently high levels of ozone in the future under the SSP3–70 scenario. This is particularly worrying for South Asia, a region where food security is a real issue and where it has been shown that significant crop losses already occur because of ozone damage [45]. This is an important region of the world for surface ozone, but a region where a lack of observations hampers our understanding of the processes that control it at the local and regional scale [41]. While it is not clear if the SSP3–70 scenario represents a likely scenario for the future, it clearly represents a scenario that should be considered from a risk assessment perspective [19]. Furthermore, we note that the changes presented in figure 3 are averaged over the geographical areas analysed. When weighted by population which is also projected to change dramatically based on the SSP scenario [46] (not shown), these changes in ozone are magnified by a further 30–50%. However, we note that our choice of annual average ozone may be a poor metric when considering ozone impacts and may underestimate future impacts of emissions and climate change. Thus, we recommend further work focuses on understanding the human health risks associated with increases in ozone under the SSP3–70 scenario to help inform policies which are informed by not only the need for ozone precursor emission control but also climate change mitigation.

By comparing the results of the UKESM1 model with the HTAP_Param (figure 4), we have shown the first-order importance of non-ozone precursor emission terms to the evolution of

ozone at 2100. Attributing the role of these non-emission terms should be the focus of follow-up studies. In particular, work attributing the role of the stratosphere on surface ozone changes should be prioritized. Over the twenty-first century we are likely to see a significant recovery of the stratospheric ozone layer—depending on the trajectory of greenhouse gases we follow we are likely to see some super recovery [47]. Coupled with increases in the strength of the global circulation driven by climate change these changes could lead to the stratosphere playing a major role on increases in ozone at the surface across the globe. There is evidence from model simulations for this (e.g. [43]) but more work is needed in this area.

Based on the performance of the HTAP_Param against the UKESM1 simulations we recommend that further work incorporates a climate scenario term to help improve the performance of the model, and its use in policy support, for situations under high levels of climate change as we have assessed here. Our results from different chemical mechanisms being run at different temperatures also point to an inherent uncertainty in the response of ozone to changes in temperature in the current generation chemistry climate and Earth system models. The comparison of two mechanisms used in global chemistry-climate and Earth system models shows that for the important VOC isoprene the two mechanisms have contrasting ozone-temperature sensitivities. Uncertainty in the mechanistic representation of isoprene chemistry is a long-standing issue for reduced chemical mechanisms and several studies have shown the impacts of this uncertainty on ozone are large (e.g. Squire *et al.* [32]) and that reconciling these mechanisms with laboratory data has significant impacts on ozone [48]. Archibald *et al.* [31] investigated the role of changes in isoprene and NOx emissions on ozone in the UKCA and MOZART-4 mechanisms along with several other mechanisms used in chemical transport models. They found an important role for the mechanistic details of isoprene peroxy radicals but failed to investigate the impacts of changes in temperature on the spread of modelled ozone. Here we show for the first time with these types of mechanisms, that in addition to uncertainty in the response of ozone to changes in VOCs and NOx, there is inherent uncertainty in the response of ozone to changes in temperature too. This clearly provides an extra challenge for mechanism developers but also for the laboratory community who tend to perform the majority of their studies at room temperature [49].

The spread in projections of future ozone at the global scale shows that there is a large amount of uncertainty in what could happen. However, the relatively short lifetime of ozone in the troposphere enables rapid changes in its precursor emissions to have significant effects (figure 3). As we write this manuscript the atmosphere is undergoing a huge experiment driven by global scale reductions in the emissions of ozone-precursors as a result of the COVID-19 global pandemic. Understanding how the atmosphere responds to these emission changes is crucial to helping to provide more confidence in the types of model simulations we have analysed here. We feel there is strong motivation to avoid scenarios like SSP3–70 but this will require continued global coordination and could be threatened by post-pandemic economic recovery deals which do not recognize the importance of air quality and climate change.

References

1. Monks PS *et al.* 2015 Tropospheric ozone and its precursors from the urban to the global scale from air quality to short-lived climate forcer. *Atmos. Chem. Phys.* **15**, 8889–8973. (doi:10.5194/acp-15-8889-2015)

2. Apling AJ, Sullivan EJ, Williams ML, Ball DJ, Bernard RE, Derwent RG, Eggleton AEJ, Hampton L, Waller RE. 1977 Ozone concentrations in south-east England during the summer of 1976. *Nature* **269**, 569–573. (doi:10.1038/269569a0)

3. Rasmussen DJ, Fiore AM, Naik V, Horowitz LW, McGinnis SJ, Schultz MG. 2012 Surface ozone-temperature relationships in the eastern US: a monthly climatology for evaluating chemistry-climate models. *Atmos. Environ.* **47**, 142–153. (doi:10.1016/j.atmosenv.2011.11.021)

4. Lee JD *et al.* 2006 Ozone photochemistry and elevated isoprene during the UK heatwave of August 2003. *Atmos. Environ.* **40**, 7598–7613. (doi:10.1016/j.atmosenv.2006.06.057)

5. Yan Y, Pozzer A, Ojha N, Lin J, Lelieveld J. 2018 Analysis of European ozone trends in the period 1995–2014. *Atmos. Chem. Phys.* **18**, 5589. (doi:10.5194/acp-18-5589-2018)

6. Lin M, Horowitz LW, Payton R, Fiore AM, Tonnesen G. 2017 US surface ozone trends and extremes from 1980 to 2014: quantifying the roles of rising Asian emissions, domestic controls, wildfires, and climate. *Atmos. Chem. Phys.* **17**, 2943–2970. (doi:10.5194/acp-17-2943-2017)

7. Hoesly RM *et al.* 2018 Historical (1750–2014) anthropogenic emissions of reactive gases and aerosols from the Community Emissions Data System (CEDS). *Geosci. Model Dev.* **11**, 369–408. (doi:10.5194/gmd-11-369-2018)

8. Fu TM, Tian H. 2019 Climate change penalty to ozone air quality: review of current understandings and knowledge gaps. *Curr. Pollut. Rep.* **5**, 159–171. (doi:10.1007/s40726-019-00115-6)

9. Porter WC, Heald CL. 2019 The mechanisms and meteorological drivers of the summertime ozone–temperature relationship. *Atmos. Chem. Phys.* **19**, 13 367–13 381. (doi:10.5194/acp-19-13367-2019)

10. Seinfeld JH, Pandis SN. 2016 *Atmospheric chemistry and physics: from air pollution to climate change*. Hoboken, NJ: John Wiley & Sons.

11. Atkins PW, De Paula J, Keeler J. 2018 *Atkins' physical chemistry*. Oxford, UK: Oxford University Press.

12. Revell LE, Williamson BE. 2013 Why are some reactions slower at higher temperatures? *J. Chem. Educ.* **90**, 1024–1027. (doi:10.1021/ed400086w)

13. McGillen MR, Baasandorj M, Burkholder JB. 2013 Gas-phase rate coefficients for the OH+ n-, i-, s-, and t-butanol reactions measured between 220 and 380 K: Non-Arrhenius behavior and site-specific reactivity. *J. Phys. Chem. A* **117**, 4636–4656. (doi:10.1021/jp402702u)

14. Atkinson R, Baulch DL, Cox RA, Crowley JN, Hampson RF, Hynes RG, Jenkin ME, Rossi MJ, Troe J. 2004 Evaluated kinetic and photochemical data for atmospheric chemistry: volume I - gas phase reactions of O_x, HO_x, NO_x and SO_x species. *J. Atmos. Chem. Phys* **4**, 1461–1738. (doi:10.5194/acp-4-1461-2004)

15. Fischer EV *et al.* 2014 Atmospheric peroxyacetyl nitrate (PAN): a global budget and source attribution. *Atmos. Chem. Phys.* **14**, 2679–2698. (doi:10.5194/acp-14-2679-2014)

16. Khan MAH, Cooke MC, Utembe SR, Archibald AT, Derwent RG, Jenkin ME, Leather KE, Percival CJ, Shallcross DE. 2017 Global budget and distribution of peroxyacetyl nitrate (PAN) for present and preindustrial scenarios. *Int. J. Earth Environ. Sci.* **2**, 2:IJEES-130. (doi:10.15344/2456-351x/2017/130)

17. Guenther AB, Jiang X, Heald CL, Sakulyanontvittaya T, Duhl T, Emmons LK, Wang X. 2012 The model of emissions of gases and aerosols from nature version 2.1 (MEGAN2.1): an extended and updated framework for modeling biogenic emissions. *Geosci. Model Dev.* **5**, 1471–1492. (doi:10.5194/gmd-5-1471-2012)

18. Rubin JI, Kean AJ, Harley RA, Millet DB, Goldstein AH. 2006 Temperature dependence of volatile organic compound evaporative emissions from motor vehicles. *J. Geophys. Res. Atmos.* **111**, D3. (doi:10.1029/2005JD006458)

19. Sutton R. 2019 Climate science needs to take risk assessment much more seriously. *Bull. Am. Meteorol. Soc.* **100**, 1637–1642. (doi:10.1175/BAMS-D-18-0280.1)
20. Sellar AA *et al.* 2019 UKESM1: description and evaluation of the UK earth system model. *J. Adv. Model. Earth Syst.* **11**, 4513–4558. (doi:10.1029/2019MS001739)
21. Eyring V, Bony S, Meehl GA, Senior CA, Stevens B, Stouffer RJ, Taylor KE. 2016 Overview of the coupled model intercomparison project phase 6 (CMIP6) experimental design and organization. *Geosci. Model Dev.* **9**, 1937–1958. (doi:10.5194/gmd-9-1937-2016)
22. Turnock ST *et al.* 2018 The impact of future emission policies on tropospheric ozone using a parameterised approach. *Atmos. Chem. Phys.* **18**, 8953–8978. (doi:10.5194/acp-18-8953-2018)
23. Turnock ST, Wild O, Sellar A, O'Connor FM. 2019 300 years of tropospheric ozone changes using CMIP6 scenarios with a parameterised approach. *Atmos. Environ.* **213**, 686–698. (doi:10.1016/j.atmosenv.2019.07.001)
24. Archibald AT *et al.* 2020 Description and evaluation of the UKCA stratosphere–troposphere chemistry scheme (StratTrop vn 1.0) implemented in UKESM1. *Geosci. Model Develop.* **13**, 1223–1266. (doi:10.5194/gmd-13-1223-2020)
25. Sellar AA *et al.* 2020 Implementation of UK Earth system models for CMIP6. *J. Adv. Model. Earth Syst.* **12**, e2019MS001946. (doi:10.1029/2019MS001946)
26. O'Neill BC *et al.* 2016 The scenario model intercomparison project (ScenarioMIP) for CMIP6. *Geosci. Model Dev.* **9**, 3461–3482. (doi:10.5194/gmd-9-3461-2016)
27. Koffi B, Dentener F, Janssens-Maenhout G, Guizzardi D, Crippa M, Diehl T, Galmarini S, Solazzo E. 2016 Hemispheric Transport Air Pollution (HTAP): Specification of the HTAP2 experiments–Ensuring harmonized modelling. EUR 28255 EN–Scientific and Technical Research Reports.
28. Young *et al.* 2013 Pre-industrial to end 21st century projections of tropospheric ozone from the Atmospheric Chemistry and Climate Model Intercomparison Project (ACCMIP). *Atmos. Chem. Phys.* **13**, 2063–2090. (doi:10.5194/acp-13-2063-2013)
29. Young *et al.* 2018 Tropospheric Ozone Assessment Report: Assessment of global-scale model performance for global and regional ozone distributions, variability, and trends. *Elementa-Sci. Anthrop.* **6**(1).
30. Wild O, Voulgarakis A, O'Connor F, Lamarque J-F, Ryan EM, Lee L. 2020 Global sensitivity analysis of chemistry–climate model budgets of tropospheric ozone and OH: exploring model diversity. *Atmos. Chem. Phys.* **20**, 4047–4058. (doi:10.5194/acp-20-4047-2020)
31. Archibald AT, Jenkin ME, Shallcross DE. 2010 An isoprene mechanism intercomparison. *Atmos. Environ.* **44**, 5356–5364. (doi:10.1016/j.atmosenv.2009.09.016)
32. Squire OJ, Archibald AT, Griffiths PT, Jenkin ME, Smith D, Pyle JA. 2015 Influence of isoprene chemical mechanism on modelled changes in tropospheric ozone due to climate and land use over the 21st century. *Atmos. Chem. Phys.* **15**, 5123–5143. (doi:10.5194/acp-15-5123-2015)
33. Knote C *et al.* 2015 Influence of the choice of gas-phase mechanism on predictions of key gaseous pollutants during the AQMEII phase-2 intercomparison. *Atmos. Environ.* **115**, 553–568. (doi:10.1016/j.atmosenv.2014.11.066)
34. Knote C, Barré J, Eckl M. 2018 BEATBOX v1.0: background error analysis testbed with box models. *Geosci. Model Dev.* **11**, 561–573. (doi:10.5194/gmd-11-561-2018)
35. Emmons LK *et al.* 2010 Description and evaluation of the model for ozone and related chemical tracers, version 4 (MOZART-4). *Geosci. Model Dev.* **3**, 43–67. (doi:10.5194/gmd-3-43-2010)
36. Griffiths PT *et al.* 2020 Tropospheric ozone in CMIP6 Simulations. *Atmos. Chem. Phys. Discuss.* **20**, 1–50. (doi:10.5194/acp-2019-1216)
37. Schultz MG *et al.* 2017 Tropospheric ozone assessment report: database and metrics data of global surface ozone observations. *Elementa: Sci. Anthropocene* **5**, 58. (doi:10.1525/elementa.244)
38. Turnock ST *et al.* 2020 Historical and future changes in air pollutants from CMIP6 models. *Atmos. Chem. Phys. Discuss.* **20**, 1–40.
39. Schnell JL *et al.* 2015 Use of North American and European air quality networks to evaluate global chemistry–climate modeling of surface ozone. *Atmos. Chem. Phys.* **15**, 10581–10596. (doi:10.5194/acp-15-10581-2015)
40. Forster PM, Maycock AC, McKenna CM, Smith CJ. 2020 Latest climate models confirm need for urgent mitigation. *Nat. Clim. Change* **10**, 7–10. (doi:10.1038/s41558-019-0660-0)
41. Hakim ZQ, Archer-Nicholls S, Beig G, Folberth GA, Sudo K, Abraham NL, Ghude S, Henze DK, Archibald AT. 2019 Evaluation of tropospheric ozone and ozone precursors in

simulations from the HTAPII and CCMI model intercomparisons – a focus on the Indian subcontinent. *Atmos. Chem. Phys.* **19**, 6437–6458. (doi:10.5194/acp-19-6437-2019)

42. Archibald AT *et al.* 2020 Tropospheric Ozone Assessment Report: Critical review of changes in the tropospheric ozone burden and budget from 1960–2100. Submitted Elementa, 2020.

43. Abalos M *et al.* 2019 Future trends in stratosphere-to-troposphere transport in CCMI models. *Atmos. Chem. Phys. Discuss.* **20**, 6883–6901. (doi:10.5194/acp-20-6883-2020)

44. Doherty RM *et al.* 2013 Impacts of climate change on surface ozone and intercontinental ozone pollution: a multi-model study. *J. Geophys. Res. Atmospheres* **118**, 3744–3763. (doi:10.1002/jgrd.50266)

45. Ghude SD, Jena C, Chate DM, Beig G, Pfister GG, Kumar R, Ramanathan V. 2014 Reductions in India's crop yield due to ozone. *Geophys. Res. Lett.* **41**, 5685–5691. (doi:10.1002/2014GL060930)

46. O'Neill BC, Kriegler E, Riahi K, Ebi KL, Hallegatte S, Carter TR, Mathur R, van Vuuren DP. 2014 A new scenario framework for climate change research: the concept of shared socioeconomic pathways. *Clim. Change* **122**, 387–400. (doi:10.1007/s10584-013-0905-2)

47. Eyring V *et al.* 2010 Multi-model assessment of stratospheric ozone return dates and ozone recovery in CCMVal-2 models. *Atmos. Chem. Phys.* **10**, 9451–9472. (doi:10.5194/acp-10-9451-2010)

48. Schwantes RH *et al.* 2020 Comprehensive isoprene and terpene gas-phase chemistry improves simulated surface ozone in the southeastern US. *Atmos. Chem. Phys.* **20**, 3739–3776. (doi:10.5194/acp-20-3739-2020)

49. McGillen MR, Carter WPL, Mellouki A, Orlando JJ, Picquet-Varrault B, Wallington TJ. 2020 Database for the kinetics of the gas-phase atmospheric reactions of organic compounds. *Earth Syst. Sci. Data* **12**, 1203–1216. (doi:10.5194/essd-12-1203-2020)